Academia Journal of Biotechnology 10(8): 133-139, August 2022
DOI: 10.15413/ajb.2022.0101
ISSN 2315-7747

Academia Publishing

Research Paper

Wear performance of WC powder cladded on steel surface using Gas Tungsten Arc Welding

Accepted 14th January 2022

De-Xing Peng

Department of Vehicle Engineering, Army Academy, Taiwan, R.O.C.

*Corresponding author. E-mail: sugarest.tw@gmail.com

ABSTRACT

This study evaluated the wear performance of carbon steel cladded with WC powders through gas tungsten arc welding. The wear behaviors of different cladding specimens were evaluated using a rotating-type tribometer under dry-sliding conditions. The cladding microstructures were characterized through optical microscopy (OM), scanning electron microscopy (SEM), and X-ray energy dispersive spectroscopy (EDS). The experimental results confirmed that the hardness of the cladded carbon steel was considerably higher than that of the carbon steel without cladding. The wear scar area of the specimen with WC cladding was only one-tenth that of carbon steel without cladding.

Key words: Gas tungsten arc welding, cladded, WC.

INTRODUCTION

Cladding is defined as the deposition of a dissimilar material on a substrate surface by applying heat sources such as arcs, flames, induction heat, and high energy beams to obtain desired properties (Wang et al., 2008). Ceramics generally have a higher wear resistance compared with metallic materials because of their high hardness. Thus, cladding metallic substrates with a ceramic or a ceramic-reinforced metal matrix composite (MMC) layer substantially prolongs the service life of metallic components in abrasive or erosive environments. Cladding with a composite coating that contains ceramic particles (e.g., WC, TiC, TiN, SiC, ZrO2, or Al2O3 ceramics) applies the direct injection of powder into a melt pool, which is formed at the substrate surface by using a laser beam(Lu et al., 2004; Xu et al., 2006). Carbon steel is widely used in mechanical components and structures; however, its wear performance is poor. Surface cladding is a major method of improving the wear performance of carbon steel (Lin and Wang, 2008). Ceramic materials are widely used in surface cladding, especially to improve the wear performance of surfaces. They also improve the wear and corrosion resistance of mechanical elements without affecting the internal properties. WC particles have attracted considerable interest due to their excellent physical and chemical properties. Because of its high hardness (3000–4000HV) and stability at high temperatures, WC is widely used in wear-resistant coatings. Application of WC particles in carbon steel claddings is now an essential research topic. WC particles are effective for improving the tribological properties of carbon steel because of their high melting point, low density, and favorable thermal and chemical stability (Lin and Wang, 2004).

Microstructure surfaces and compositions are crucial factors in wear resistance. Therefore, controlling and minimizing wear are the major objectives of coating research and technology (Wang et al., 2002; Chen and Wang, 2004). Gas tungsten arc welding (GTAW) cladding is an effective surface modification technique that provides sufficient engineering thickness and excellent bonding with the substrate (Chen and Wang, 2003; Wang et al., 2008). This technique has evolved from simple cladding to composite cladding in which compounds with high-melting-point and high-hardness, such as carbides, nitrides, and borides, are added to the cladding (Wang et al., 2004). A key characteristic of GTAW cladding is rapid solidification, which produces extremely fine and novel microstructures (Wu et al., 2004; Wang et al., 2003). Recently, GTAW has been successfullyappliedfor surface modification. The

Table 1: Composition of the AISI 1020 substrate

Element	C	Si	Mn	P	S	Cr	Fe
wt.%	0.22	0.22	0.55	0.01	0.009	0.15	98.84

advantages of GTAW are technical simplicity, low cost, and a strong metallurgical bond between the cladding layer and substrate. Therefore, this technology is widely used for surface cladding and alloying, which can considerably improve wear performance (Man et al., 2006).

Axen (1992) studied the abrasive wear behavior of steel tools cladded with a TiC–steel composite layer. The experimental results indicated that the abrasive wear resistance was considerably influenced by the size of the reinforcing TiC particles, matrix hardness, retained austenite and abrasive grit size. Lin (2003) studied a TiC alloy composite coating clad onto a 1045 steel substrate. The microstructural constituents of the cladded layer exhibited TiC in the dendrites. The TiC particles significantly enhanced the wear resistance and the severity of wear depended mainly on the debonding removal of the particles. From a tribological perspective, such claddings provide excellent abrasive wear resistance because of the high hardness of WC. Therefore, this study investigated the wear performance of ceramic metal cladding layers produced by cladding ceramic powders on carbon steel through GTAW. The effects of the hardness of the cladding layer, microstructure, various cladding powder compositions, applied loads, and sliding time were evaluated. Cladding microstructures were characterized using an optical microscope, scanning electron microscope (SEM), and X-ray energy-dispersive spectrometer (EDS). Cladding wear resistance was evaluated under room-temperature block-on-ring dry sliding wear conditions, and the corresponding wear mechanisms were analyzed.

METHODOLOGY

Materials used

Carbon steel samples were machined into 20×10×70mm^3 rectangular blocks before being used as substrate materials. Table 1 gives the chemical composition of the substrate. Before cladding, the surface was ground to a Ravalue of 0.2 μm and cleaned with acetone in an ultrasonic cleaner for 10 min. WC particles (size 10–50 μm) were initially used as the reinforcing phase.

The cladding procedure

The first step of the cladding process was to prepare cladding materials by filling 316 stainless steel tubes with powders. Table 2 lists the chemical compositions of the 316 stainless steel tubes. After the filling of the 316 stainless steel tubes with the cladded powders, each tube was rolled to a size of 1.2 ×3.5 ×60 mm^3 and then fixed to the substrate surface. Finally, cladding was performed using GTAW. Claddings were prepared using a tungsten inert gas (TIG) welding machine. Figure 1 illustrates the TIG welding process. Table 3 shows the conditions of the cladding process.

Investigations and tests of the claddings

Metallographic samples of composite claddings were prepared using standard mechanical polishing procedures and were etched in H2SO4:HCl:HNO3 water solution in a volume ratio of 15:3:2. The microstructure and composition distribution were examined under a field-emission SEM and EDS, respectively.

Wear tests

A block-on-ring rotating wear test machine was used for wear testing at room temperature without lubrication (Figure 2). Frictional pairs were formed by forcing a stationary block against a rotating ring. The claddings were ground before testing to obtain a smooth surface (Ra = 0.35μm). The ring was made of bearing steel and had a diameter of 70 mm and height of 18.7 mm. Table 4 lists the wear test conditions. The friction torque was measured within a 1-sec interval by using a torque-measuring system, and the friction coefficient was obtained through calculations. After the wear test, the specimens were immediately rinsed in ethanol. The topography of the scar surfaces was then observed through SEM.

RESULTS AND DISCUSSION

Microstructure and hardness distribution of the clad layers

The microstructure of the substrate metal was examined before the microstructure of the cladding. Figure 3 displays the optical micrograph of carbon steel in the annealed condition. As shown, carbon steel predominantly exhibited a ferritic microstructure and a small fraction of pearlite areas at the boundaries. For most applications, the bonding strength of reinforcement interfaces is an essential factor in the performance of the cladding layer. Figure 4 displays a

Table 2: Composition of 316 stainless steel tubes

Element	C	Mn	Cr	Ni	Mo	Fe
wt.%	0.08	2.0	17	12	3	65.92

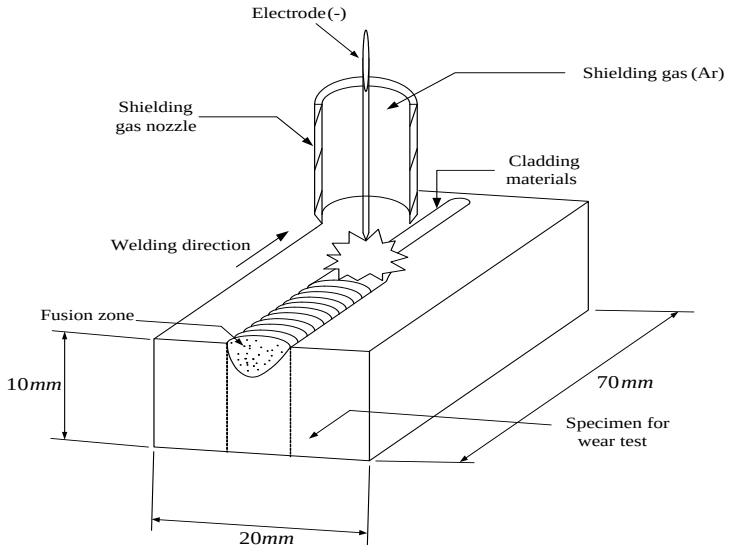

Figure 1: Schematic representation of the weld cladding

Table 3: Welding parameters (gas tungsten arc welding process)

Welding current (A)	150
Welding speed (cm/min)	10
Electrode	W–2% thorium
Arc gap (mm)	1.5
Torch position	Vertical
Shield gas	Argon, flow rate (8 ℓ /min)

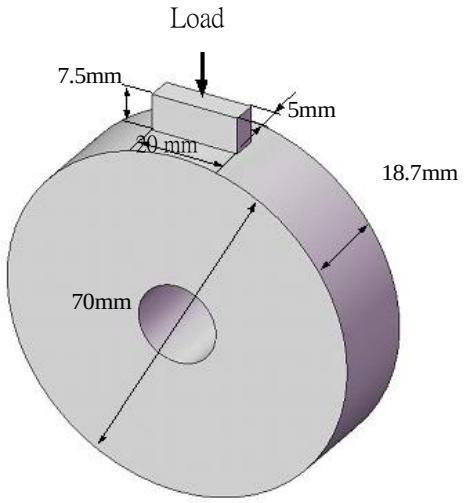

Figure 2: Schematic illustration of the block-on-ring sliding tester

Table 4: Wear test conditions

Apparent load (N)	50/100/125/150
Sliding speed (m/s)	1.83
Sliding distance (m)	3297/6594/9891/13188
Temperature	Room temperature

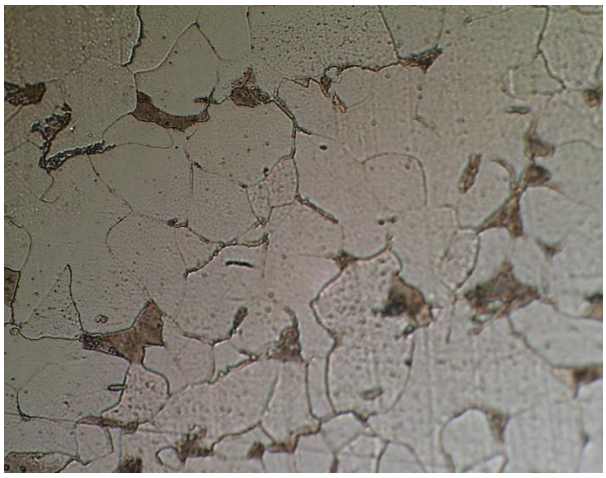

Figure 3: Optical micrograph showing the microstructure of the carbon steel substrate

Figure 4: Morphology of the GTAW-clad coating

micrograph of the bonding region between the cladding and substrate. The macrographs exhibited a continuous and uniform appearance with no cracks and porosity. The high electrical current of the cladding caused the flat and wide appearance of the cladding surface. For each pass, the width of the cladding layer was approximately 8 mm and the depth of the melting pool was approximately 3 mm. A thick cladding layer was obtained using a high welding current and low welding speed. The cladding obtained was of high quality. Moreover, an excellent metallurgical bond was established between the cladding and substrate. Figure 5 displays the EDS results.

The EDS results indicate that cubic and dendrite-shaped phases were rich in WC, and Cr. Moreover, Fe-rich phases were detected only in the matrix. Only tungsten was detected in the white phases, which indicated that these phases were tungsten carbide. Because WC is relatively harder than α ferrite, it improved the wear resistance of the claddings. Micro-hardness measurements were performed to assess the hardness distribution across clad beads. Figure 6 presents the variation in hardness between the surface and substrate in a cladding layer. The GTAW cladding zone had significantly higher hardness than did the unreinforced carbon steel substrate (200Hv). This large increase in hardness could be attributed to the presence of WC and the change in hardness was consistent with the graded is tribute on o the hard WC phase in the matrix. Notably, the observed micro-hardness within the coating gradually decreased from the top surface to the bottom. The WC particles were typically segregated to the upper regions in the coating because of the low density of WC, which produced a macroscale gradient distribution.

Wear behavior of the clad specimens

Figure 7 shows the variation in the wear scar area of the original carbon steel and in the WC-reinforced intermetallic

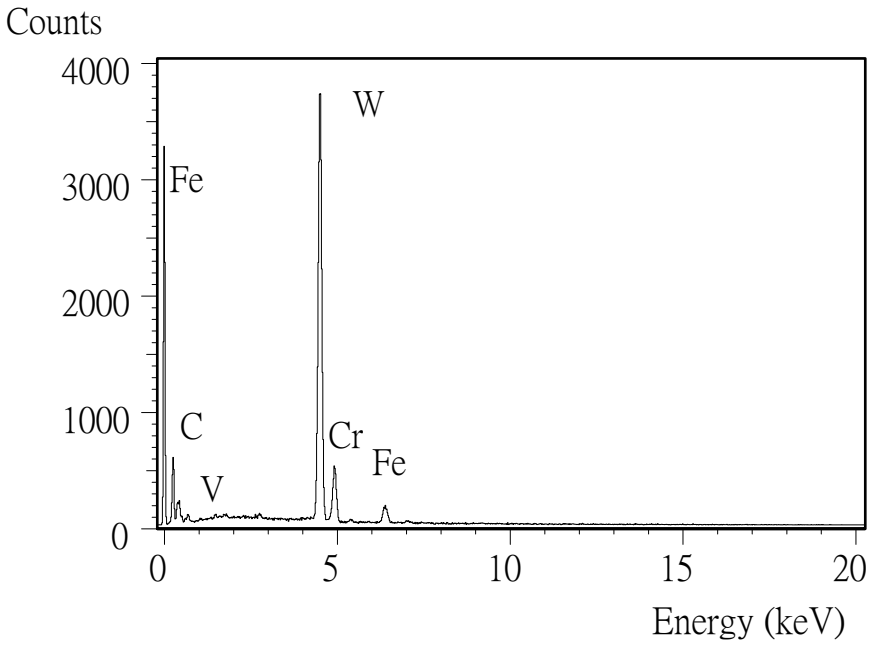

Figure 5:EDS spectra of the WC clad layer

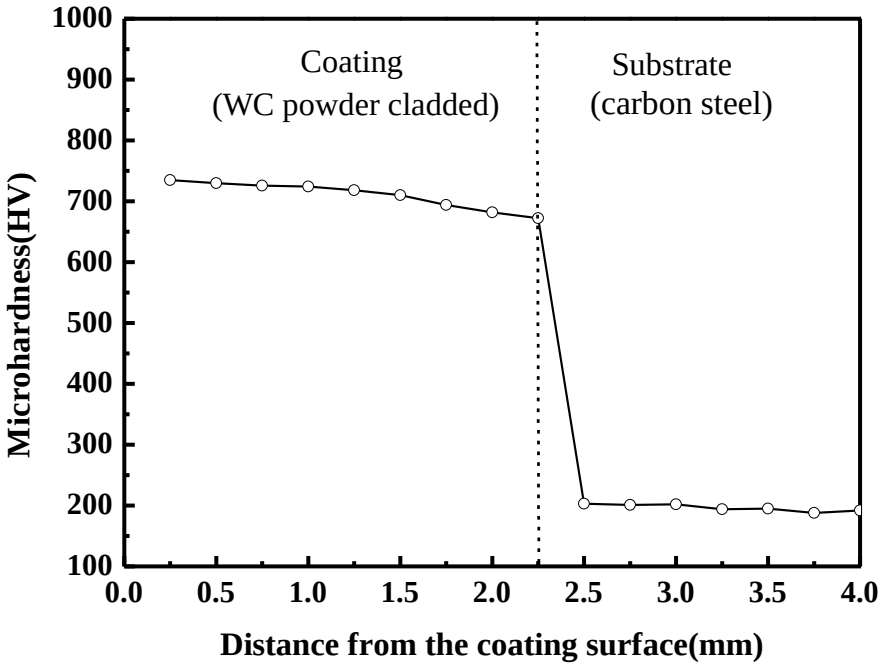

Figure 6: Micro-hardness profile along the cross-section of the coating

composite coating under varying test loads. The scarring of the intermetallic coating slowly increased with the test load, whereas the scarring of the original carbon steel rapidly increased with the test load. Surface fractures occurred at a maximum load of 100 N because of adhesive wear. This observation implies that the WC-reinforced wear-resistant coating was unaffected by the applied load, and its anti-wear performance was thus considerably superior to that of the original carbon steel under heavy loading tribological service conditions. In the GTAW-cladded WC wear-resistant intermetallic composite coating, the hardness and wear resistance of the WC primary phases were uniformly distributed in the matrix. The unique microstructureof the GTAW-claddedintermetallic

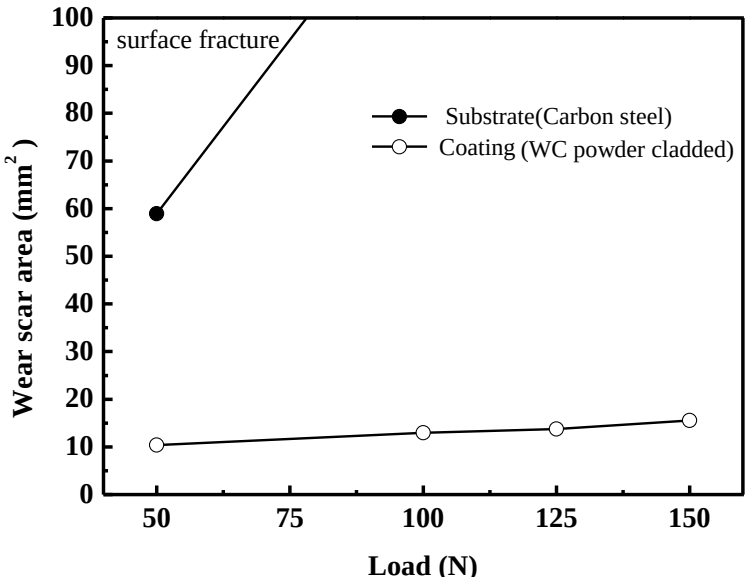

Figure 7: Wear scar area of substrate and the GTAW clad coating as a function of test load at a given wear time of 2 h

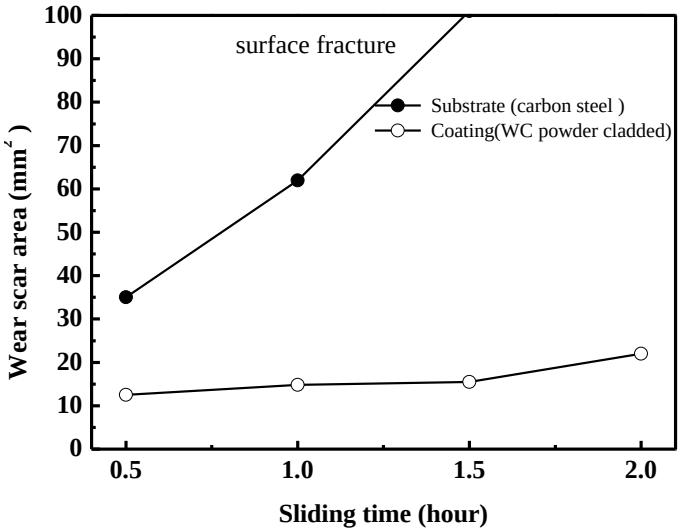

Figure 8: Wear scar area of the coating and the substrate as function of wear time at a given normal load of 100 N

composite coating exhibited excellent wear resistance, particularly under heavy loading conditions. Figure 8 compares the wear observed on the WC coating with that observed on carbon steel as a function of wear time under a normal load (100N). The relationship between the wear scar area and wear time was approximately linear, and the slope for carbon steel was evidently greater than that for the WC coating.

CONCLUSION

The following conclusions were drawn from the study:

1. A WC-cladded layer can form an appropriate metallurgical bond with its substrate and exhibits uniform dispersion of WC particulates in the cladding surface.
2. A GTAW cladding has a homogenous microstructure, suitable metallurgical bond with its substrate, and uniform dispersion of WC particulates in its cladding surface.
3. In this study, the hardness increased from HRv 200 in the original carbon steel to HRv 700 in the carbon steel clad with WC particles.
4. Coatings reinforced with WC particles exhibited higher wear resistance and a lower friction coefficient than did the substrate because the uniform distribution of hard compound particles in the matrix improved the wear

resistance of the cladding.

REFERENCES

Chen Y, Wang HM (2004). " High-temperature wear resistance of a laser clad TiC reinforced FeAl in situ composite coating," Surf. Coat. Technol. 179: 252-256.

Chen Y, Wang HM (2003). "Microstructure and wear resistance of laser clad TiC reinforced FeAl intermetallic matrix composite coatings," Surf. Coat. Technol. 168: 30-36.

Lin YC, Chang KY (2010). Elucidating the microstructure and wear behavior of .multi-passcladding on AISI 1050 steel. J. Mater. Process. Technol. 210: 219–225.

Lin YC, Cho YH (2008). "Elucidating the microstructure and wear behavior for multicomponent alloy clad layers by in situ synthesis," Surf. Coat. Technol. 202: 4666–4672

Lin YC, Wang SW (2004). Microstructure of TiC–W cladding on steel in nanoscale Wear 256: 720–725

Lin YC, Wang SW (2003). "Wear behavior of ceramic powder cladding on an S50C steel surface", Tribol. Int. 36: 1-9.

Lin YC, Wang SW (2003). "Wear behavior of ceramic powder cladding on an S50C steel surface," Tribol. Int. 36: 1-9.

Lin YC, Wang SW, Wu KE (2003). "The wear behaviour of machine tool guideways clad with W-Ni, W-Co and W-Cu using gas tungsten arc welding," Surf. Coat. Technol. 172: 158-165.

Lu SP, Kwon OY, Kim TB, Kim KH (2004). "Microstructure and wear property of Fe-Mn-Cr-Mo-V alloy cladding by submerged arc welding," J. Mater. Process. Technol. 147: 191-196.

Man HC, Zhang S, Cheng FT, Guo X (2006). "In situ formation of a TiN/Ti metal matrix composite gradient coating on NiTi by laser cladding and nitriding," Surf. Coat. Technol. 200: 4961-4966.

Wang SW, Lin YC, Tsai YY (2003). "The effects of various ceramic-metal on wear performance of clad layer," Mater. Process. Technol. 140: 682-687.

Wang X, Zhang M, Zou Z, Qu S (2002). "Microstructure and properties of laser clad TiC + NiCrBSi + rare earth composite coatings," Surf. Coat. Technol. 161:195-199.

Wang XH, Zhang M, Liu XM, Qu SY, Zou ZD (2008). "Microstructure and wear properties of TiC/FeCrBSi surface composite coating prepared by laser cladding," Surf. Coat. Technol. 202:3600-3906.

Wang Y, Wang HM (2004). "Wear resistance of laser clad Ti2Ni3Si reinforced intermetallic composite coatings on titanium alloy," Appl. Surf. Sci. 229: 81-86.

Wang ZT, Zhou XH, Zhao GG (2008). "Microstructure and formation mechanism of in-situ TiC-TiB2/Fe composite coating," Trans. Nonferrous Met. Soc. China 18: 831-835.

Wu P, Du HM, Chen XL, Li ZQ, Bai HL, Jiang EY (2004). "Influence of WC particle behavior on the wear resistance properties of Ni–WC composite coatings," Wear 257: 142-147,

Xu J, Liu TW, Zhong M (2006). "Microstructure and dry sliding wear behavior of MoS2/TiC/Ni composite coatings prepared by laser cladding," Surf. Coat. Technol. 200: 4277-4232.

Cite this article as:

Peng DX (2022). Wear performance of WC powder cladded on steel surface using Gas Tungsten Arc Welding. Acad. J. Biotechnol. 10(8): 133-139.

Submit your manuscript at
http://www.academiapublishing.org/ajb